NUMERICAL MODELLING OF NON-UNIFORM STEEL CORROSION DEVELOPMENT AND ITS MECHANICAL INFLUENCES ON REINFORCED CONCRETE STRUCTURES

E CHEN *, CHRISTOPHER K.Y. LEUNG†

***** Department of Civil and Environmental Engineering
The Hong Kong University of Science and Technology
Clear Water Bay, Kowloon, Hong Kong
E-mail : teresachan@ust.hk, web page: http://www.ust.hk

† Professor, Department of Civil and Environmental Engineering
The Hong Kong University of Science and Technology
Clear Water Bay, Kowloon, Hong Kong
E-mail : ckleung@ust.hk, web page: http://www.ust.hk

Key words: Non-uniform corrosion, Finite element analysis, Cover cracking, Crack width

Abstract: Steel corrosion and the associated cracking of the concrete cover can significantly reduce the service life of reinforced concrete (RC) structures. In most studies on corrosion-induced cracking, the distribution of rust was assumed to be uniform around the steel bar. However, under practical situations, steel reinforcement corrosion should start at the position nearest to the exposed surface and gradually spreads to other parts along its circumference. As a result, the chloride attack-penetration and the build-up of rust around the bar are far from being uniform. The present work will focus on non-uniform corrosion due to chloride penetration. The time-varying corrosion penetration around the rebar is first obtained by solving the diffusion equation numerically by Matlab. In the calculation, corrosion is assumed to initiate at a point when a specified chloride threshold value is reached at that position. The effects of cover thickness and corrosion rate on the non-uniformity of corrosion penetration are studied.

To analyze crack propagation in the concrete cover due to rust expansion, the numerically formed shapes of rust and corroded steel configuration at different corrosion levels are employed in the finite element analysis. Discrete crack model is adopted to simulate the crack propagation in concrete. The surface crack width evolution with increasing corrosion level is examined for both non-uniform and uniform corrosion cases with different cover thicknesses (c/d=1 and c/d=2). It has been found that: 1) Cover cracking is more severe for non-uniform corrosion than uniform corrosion under similar percentage of steel loss. As a result, it is important to consider non-uniform corrosion in the analysis. 2) For larger cover thickness, the initiation of surface cracking is delayed, but its width becomes larger for the same amount of steel loss after surface cracking. This finding suggests that repair work should be performed immediately if corrosion-induced surface cracks are found in locations with large cover.

1 INTRODUCTION

Steel corrosion is the main culprit impairing the durability and safety of reinforced concrete structure. When corrosion-inducing chemicals (such as chlorides) reach a threshold concentration on the steel surface, reinforcement corrosion starts to occur. Since rust has a higher volume than steel, the concrete cover will be subjected to internal pressure. With continued corrosion leading to increasing pressure, the cover will crack, making it easier for aggressive chemicals to penetrate. The corrosion process will then be accelerated. From the structural point of view, corrosion can lead to debonding between the rebar and cover, and even significant loss of steel area which affects the safety of reinforced concrete structures. Due to its great harmfulness to durability of RC structures, steel corrosion and the associated cracking process have been studied by many investigators [1-19]. The analytical and numerical models to predict corrosion induced-cracking [2-3, 6-9, 11-15] usually assumed uniform corrosion around the rebar. In experimental studies [1, 11-12], corrosion was accelerated by applying current or adding chloride into the mix, so that the distribution of rust around the steel was also uniform. The obtained results are difficult to be extended to real situations, where steel corrosion occurs earlier at locations closer to the exposed surface(s) of structure, leading to non-uniform rust distribution. Several researchers have performed experiments to study non-uniform rusting around the steel, when chlorides are penetrating from one side of the specimen. Yuan and Ji [16] observed the non-uniform corrosion distribution by SEM and EPM analysis, and fit the distribution curve with an elliptic expression. Zhao et al. [19] proposed a Gaussian function to describe the rust distribution obtained from backscattered electron imaging and image analysis. A few researchers [8, 17, 18] have conducted numerical studies on the effect of non-uniform corrosion on cover cracking. The general finding is that non-uniform corrosion can result in more severe cover cracking than uniform corrosion for a similar degree of rusting.

Former studies on cover cracking under non-uniform corrosion have made various assumptions on the distribution of rust or pressure around the reinforcement. The assumed distributions are not related to the chemical concentration which induces the corrosion process. To address such a limitation, a coupled diffusion-mechanical analysis is performed in the present work for chloride-induced steel corrosion. The chloride concentration around the steel reinforcement is derived by solving the diffusion equation. Assuming a constant corrosion rate after initiation, the rust distribution can be deduced. Finite element models are then set up to study the evolution of crack width and crack patterns at different corrosion levels. Cracking development under uniform corrosion is also studied and compared to the results under non-uniform corrosion.

2 DIFFUSION PROCESS AND NON-UNIFORM CORROSION DISTRIBUTION

In the analysis, chloride diffusion is assumed to take place in a reinforced concrete beam with its top surface exposed to constant chloride concentration. Corrosion starts to occur at a particular location when the chloride concentration reaches a critical value. By solving the diffusion equation in Matlab, the corrosion initiation time at different locations around the rebar is first calculated. Under the assumption that (i) corrosion progresses along the radial direction of the rebar, and (ii) the corrosion rate is constant, the loss of steel at any position and time can be obtained.

The non-uniformity of corrosion around the steel is also affected by cover thickness and corrosion rate, through their effects on the corrosion initiation time and material loss at different locations. In the following, these effects are investigated with the following parameters. Surface chloride concentration C_0 is taken to be 8kg/m^3, critical chloride concentration C_{crit} is 0.71kg/m^3 and the chloride diffusivity is 50mm^2/year. The diameter of steel is 20mm. For different cover thicknesses (c=20mm, 40mm, 60mm and 80mm) and corrosion rates (10μm/year, 20μm/year, 30μm/year and 50μm/year), the distribution of corrosion depth (i.e., reduction in steel radius due to corrosion) is calculated over the upper half of the steel. The relation between corrosion depth and location (in angle θ, measured from the vertical axis) around the rebar is plotted in Figure 1 and 2 to illustrate the effect of cover and corrosion rate respectively.

For the results in Figure 1, the corrosion rate is fixed at 20 μm/year. At different cover thicknesses, the corrosion initiation time will be different. Therefore, instead of comparing the corrosion depth distribution at a given time, we consider the situation when corrosion has reached a certain extent at the outermost points along the horizontal diameter (θ=+/-90^o). Specifically, Figure 1(a) shows the corrosion depth distribution when corrosion initiates at the outermost points and Figure 1(b) shows the situation when the depth is 16 μm. In both cases, the corrosion depth is found to be largest at the top of the steel bar, which is as expected. Interestingly, the corrosion depth is more non-uniform with an increasing concrete cover.

Figure 2 shows the distribution of corrosion depth for a constant cover thickness (40mm) but different corrosion rates. Figures 2a to 2c give the distribution at three different times: $t=t_{ini}$-1.0year, $t=t_{ini}$, and $t=t_{ini}$+1.0year, where t_{ini} is the corrosion initiation time at the outermost horizontal points, which is independent of corrosion rate. At a time before t_{ini} (Figure 2a), the non-uniform corrosion depth distribution is approximately Gaussian, as proposed by Zhao et al. [19] for the thickness of rust layer. (Note: this is the thickness of compressed rust layer which is not the same as the depth of corroded steel.) However, as time progresses (Figure 2b and c), the distribution looks more like a parabola. For accurate modeling of the crack-induced cracking process, the change in non-uniformity of the distribution needs to be considered.

3 FINITE ELEMENT ANALYSIS OF COVER CRACKING DUE TO NON-UNIFORM CORROSION

From diffusion process analysis in previous section, the evolution of non-uniform corroded depth distribution over time has been obtained. In this section, the non-uniform corroded steel configuration at several selected times is imported to the ATENA program for modeling the geometry at different corrosion levels. Each geometric model (corresponding to a particular rust distribution) is then analyzed individually by finite element method. The surface crack width obtained from ATENA analysis is examined for each corrosion level to trace the cover crack propagation as corrosion proceeds.

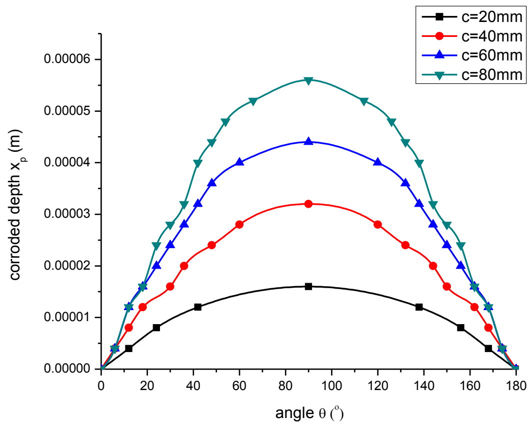

(a) when the outmost horizontal points start corrosion

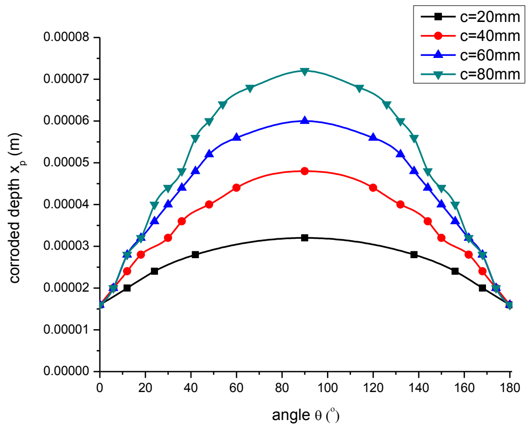

(b) when the outmost horizontal points are corroded by 16 μm

Figure 1: Corroded depth vs θ for different cover thicknesses

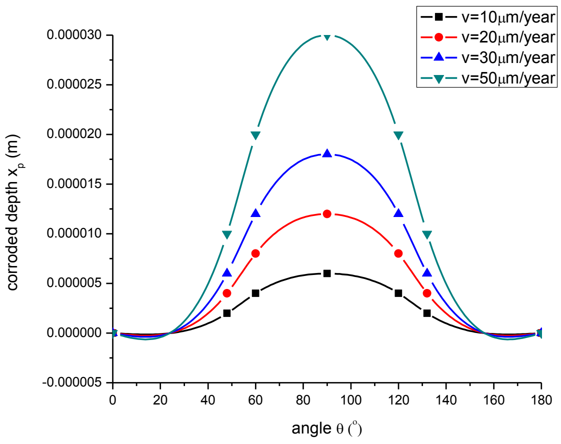

(a) t=t_ini-1.0year

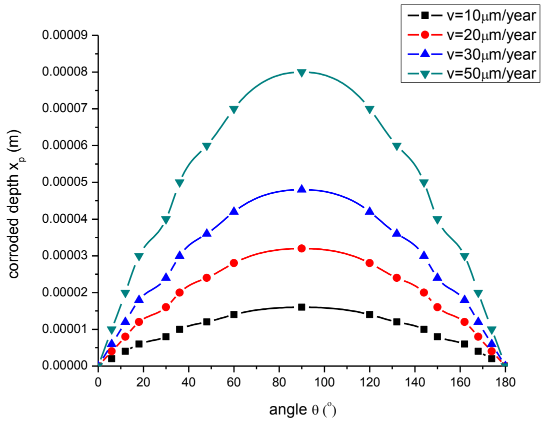

(b) t=t_ini

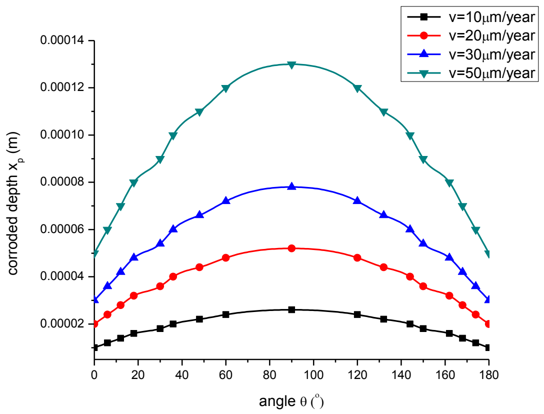

(c) t=t_ini+1.0year

Figure 2: Corroded depth vs θ for different corrosion rates

3.1 Geometry models

2-D Plain strain condition is assumed and a cross section of the RC member is modelled. The dimension of the cross section is 150mm x 150mm, with a single rebar of 20mm diameter embedded inside. Two kinds of concrete covers are modeled: 20mm and 40mm. Corrosion rate is assumed to be constant at 20μm/year. For cover thickness of 20mm, the difference of corrosion initiation time between the top of the steel bar (closest to the constant chloride boundary) and the outermost horizontal point can be easily calculated to be 0.8years, which results in 16μm difference of corrosion depth at the two locations. For cover thickness of 40mm, the difference of maximum and minimum corroded depth is 32μm. To examine the crack propagation as corrosion develops, finite element analysis is performed for different corrosion levels listed in Table 2 for cover of 20mm and Table 3 for cover of 40mm.

3.2 Rust properties and expansion

The properties of rust have been studied by several researchers [20-24]. By examining the chemical compositions of various oxides in rust and their percentage and volumetric ratio in relation to steel, Suda et al. [20] reported that the average volume of corrosion products was 3 times that of the steel. The volumetric ratios reported by other authors are not the same but in the range of 2-6. However, the elastic modulus of rust reported in the literature can be very different [22]. Molina et al. [2] simply used liquid water (which has very small elastic modulus) to represent the rust. Solgaard et al. [7] assumed 2.1GPa for rust's Young's modulus. Tran et al. [4] took 500MPa and got reasonable results. The nonlinearity behavior of rust has also been studied and used by a few researchers [9, 23]. In this study, the rust is treated as a solid elastic material with Young's modulus of 500MPa and Poisson's ratio of 0.3. The volume ratio between rust and steel is taken to be 3.

In the analysis, rust expansion is realized by giving the corroded layer an initial strain. The initial strain generated in rust under non-uniform corrosion is derived based on the theory established for uniform corrosion.

According to the cylinder model under uniform corrosion (Figure 3), the following expression can be written,

$$\boldsymbol{\pi}(\boldsymbol{r_b}+\boldsymbol{\Delta r_b})^2-\boldsymbol{\pi r_b^2}=(\boldsymbol{n}-\boldsymbol{1})\frac{\boldsymbol{w_{st}}}{\boldsymbol{\rho_{st}}}=(\boldsymbol{n}-\boldsymbol{1})[\boldsymbol{\pi r_b^2}-\boldsymbol{\pi}(\boldsymbol{r_b}-\boldsymbol{x_p})^2] \quad (1)$$

where r_b is the initial radius of the rebar, n is volume ratio of rust to steel, w_{st} is the mass of consumed steel due to corrosion, ρ_{st} is the density of steel and x_p is the radial loss of steel due to corrosion. x_p is a function of time t. If the corrosion rate v is constant and has the unit μm/year, x_p is equal to vt.

From equation (1), the free increase of rust Δr_b can be derived as,

$$\boldsymbol{\Delta r_b}=\sqrt{\boldsymbol{n r_b^2}-(\boldsymbol{r_b}-\boldsymbol{x_p})^2(\boldsymbol{n}-\boldsymbol{1})}-\boldsymbol{r_b} \quad (2)$$

The free strain of corrosion products is:

$$\boldsymbol{\varepsilon}=\frac{\boldsymbol{\Delta r_b}}{\boldsymbol{x_p}+\boldsymbol{\Delta r_b}} \quad (3)$$

From the given data in this study, the free strain is about 0.66.

For non-uniform corrosion, the penetration depth x_p (and hence Δr_b) is a function of both t and θ. Equation (1) can hence be modified to:

$$\int_0^{2\pi}\frac{1}{2}(\boldsymbol{r_b}+\boldsymbol{\Delta r_b}(\boldsymbol{\theta}))^2\,\boldsymbol{d\theta}-\boldsymbol{\pi r_b^2}=(\boldsymbol{n}-\boldsymbol{1})\left[\boldsymbol{\pi r_b^2}-\int_0^{2\pi}\frac{1}{2}(\boldsymbol{r_b}-\boldsymbol{x_p}(\boldsymbol{\theta}))^2\,\boldsymbol{d\theta}\right] \quad (4)$$

Since the expression of Δr_b in equation (2) also satisfies equation (4), it is assumed to be applicable for non-uniform corrosion. The free strain of rust can then be calculated from equation (3).

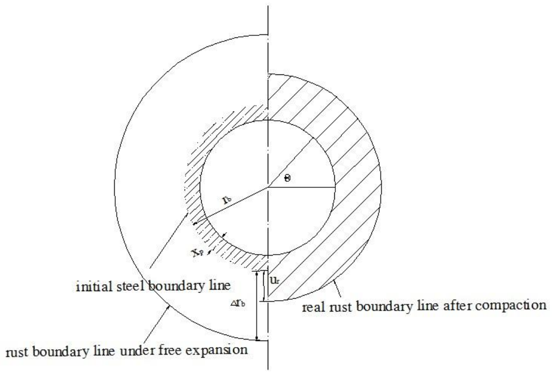

Figure 3: Deformation process due to corrosion-induced expansion

3.3 Discrete crack model

In the discrete crack model, the crack opens at a point when the stress reaches the tensile strength. The crack then transmits stress according to the cohesive law (which describes the relation between transmitted stress and crack width) as long as the crack width is less than the critical value. Using discrete crack model, the crack open phenomenon can be well captured; however, the crack path needs to be pre-defined. According to experimental observed crack patterns under rebar corrosion [1, 4, 6] and crack paths computed from smear crack models [2, 3-5, 8], the main cracks are vertical and nearly horizontal. Therefore, two vertical discrete cracks and two horizontal discrete cracks are defined in the mesh. A bilinear cohesive law is employed. With tensile strength of concrete f_t=3.2MPa and d_{max}=16mm, the other fracture parameters can be calculated from CEB-FIP model. They are presented in Figure 4 and Table 1. With discrete cracks in the mesh, the concrete can be taken as linear elastic, with Young's modulus of 36GPa and Possion's ratio of 0.2. To allow sliding, interface elements are placed between the rust and concrete elements. Properties of the interface element are given in Table 1. It is well know that rust can penetrate into pores and cracks inside the concrete, thus relieving part of the stress due to its expansion [4, 6, 11]. This will not be considered in our analysis, so the crack opening for a certain degree of corrosion will be overestimated. However, despite such a simplification in the model, the major observations and conclusions related to the development and opening of cracks, effect of concrete cover as well as the difference between uniform and non-uniform corrosion, will not be affected.

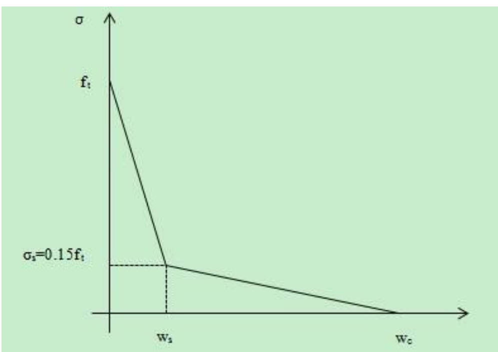

Figure 4: Bilinear cohesive law adopted in the present model

3.4 Boundary conditions and mesh of the model

Regarding the boundary conditions, the top surface and side surfaces are free. The bottom surface is supported in the vertical direction, and the left-most point is also given a support in the horizontal direction to avoid rigid body translation of the whole structure. The plane triangular element with 3 nodes is used for meshing. Figure 5 shows the mesh and the boundary conditions. A magnified mesh around the rust layer is also shown.

Table 1: Material constants in the finite element model

material	parameters	values
elastic concrete	Young's modulus	36GPa
	Poisson's ratio	0.2
rust	Young's modulus	500MPa
	Poisson's ratio	0.3
	volumetric ratio	3
steel	Young's modulus	200GPa
	Poisson's ratio	0.3
	yield strength	350MPa
	steel diameter	20mm
discrete crack	tensile strength f_t	3.2MPa
	fracture energy	0.082N/mm
	σ_s	$0.15f_t$
	w_s	0.024mm
	w_c	0.18mm
interface of concrete/rust	tensile strength	2MPa
	friction coefficient	0.2
	cohesion	1MPa

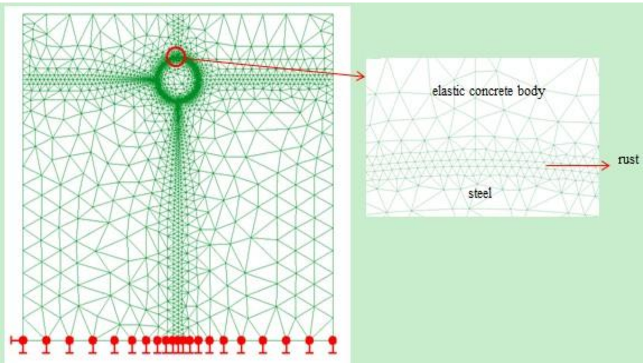

Figure 5: Geometry, meshing and boundary conditions of the model

3.5 Cover cracking process under non-uniform corrosion

The Netwon-Raphson method is used for the nonlinear analysis. The calculated initial strain is applied over a large number of load steps to achieve convergence to accurate results.

3.5.1 Cracking mechanism of concrete cover under rebar corrosion

The crack developments at different load steps are shown in Figure 6, with displacements magnified. We can see that the upper vertical discrete crack opens initially at the interior of concrete/rust interface (Figure 6(a)), and gradually propagates upwards until it suddenly opens on the top surface (Figure 6(b)). With the propagating of the horizontal cracks, the concrete cover can rotate to facilitate the opening of vertical crack (Figure 6(c)). With cover rotation, the crack width on the surface will become larger than crack width near the rust/concrete interface. Cover rotation also induces compression near the vertical surfaces, which controls the propagation and opening of the horizontal cracks.

It should be noted that the cracking mechanism discussed here refers to single rebar corrosion with free side surface, which is often the case in laboratory experiments. The main crack obtained from the present computational model is the vertical crack, which is consistent with experimental observation [1, 4]. For multi-rebar corrosion, the side surfaces should be supported horizontally with rollers if the reinforcements are symmetrically arranged. The rotation of concrete cover will then be resisted. Under such a situation, the horizontal cracks can propagate easily, open widely and causing the vertical crack to close. This is the layer debonding failure which is often observed in the field. Such a phenomenon has also been also modeled by some investigators [3, 5, 6].

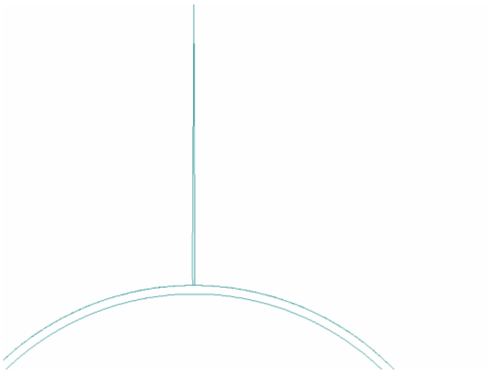

(a) The top surface has not opened yet

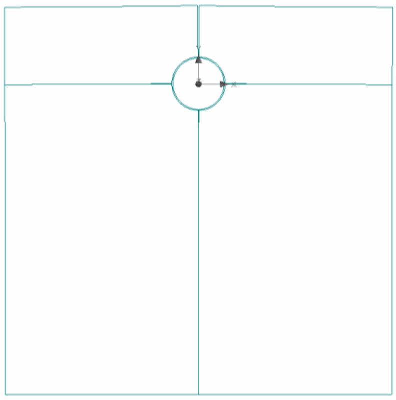

(b) The top surface has just opened

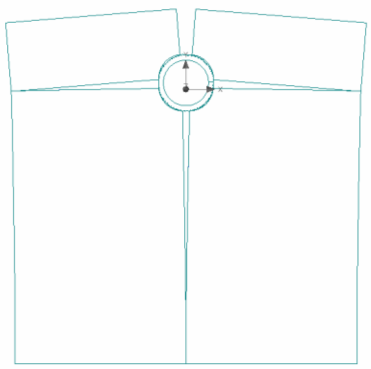

(c) The top surface crack has a large width

Figure 6: Crack developments at different load steps (The magnification is different for the above three pictures)

3.5.2 Surface crack width evolution and effect of cover thickness

The crack widths on the top surface corresponding to different corrosion levels are recorded in Table 2 and 3, for cover of 20mm and 40mm respectively. In each table, the corrosion depth is given as a range, because it varies around the circumference of the steel. With the distribution of corroded depth obtained from diffusion analysis, the corroded percentage is calculated as the ratio of corroded steel area to the initial steel area. Inspection of the results in Table 2 and 3 clearly reveals the effect of cover thickness on surface crack development. For similar corroded percentage, the surface crack opening is larger for cover of 40mm. This is because a large part of the surface crack opening is resulted from rotation of the cover (Figure 6(c)). With a thicker cover, the rotational displacement in the horizontal direction is increased. While our numerical simulation is for a laboratory specimen containing a single rebar, the same observation would apply to a rebar close to the corner of a beam (with different covers from the bottom and the side). The finding has an interesting implication to the maintenance of concrete structures. A thick cover can certainly delay corrosion initiation and crack propagation to the surface (Note: according to our computational results that are not shown in this paper, it takes a higher corroded percentage for a crack to reach the surface when the cover is thicker). However, once the surface crack is formed, its opening can increase more rapidly when the cover is thicker. Therefore, when surface cracks are observed during bridge inspection, repair should be performed immediately at locations with thick cover, to avoid delay that will allow wide opening of the crack, which can greatly accelerate the penetration of water and chlorides.

4 COMPARISON OF NON-UNIFORM AND UNIFORM CORROSION RESULTS

To compare the difference between non-uniform and uniform corrosion, finite element analysis is also performed for different penetration depths that are uniform around the steel bar. The results for cover thickness of 20mm and 40mm are given respectively in Table 2 and 3. For each penetration depth, the corroded percentage is calculated and given in the table together with the surface crack opening computed from the finite element model. The relations between crack width with corroded percentage, for the two cover thicknesses, are plotted in Figure 7 for both uniform and non-uniform corrosion. As shown in the figure, for a given corroded percentage, the crack is wider when corrosion is not uniform. Moreover, the difference between uniform and non-uniform corrosion is larger for a higher cover. This is due to the fact that the corrosion depth around the steel varies over a large range when the cover is thicker (Figure 1). When one looks at Figure 7, the difference between non-uniform and uniform cases does not seem to be very large. However, in practice, we are often interested in the degree of corrosion when the surface crack has opened to a certain value. For example, let us take 0.2mm to be the limiting crack opening. For a cover of 40mm, the corroded percentage to reach this opening is 0.45% for non-uniform corrosion. When corrosion is uniform, the required corroded percentage (from interpolation) is 0.57%. In practice, this can correspond to very different times. Therefore, for the correct determination of critical states of the corrosion process (such as a critical damage condition when the crack has opened to a certain extent), non-uniform corrosion needs to be considered.

5 CONCLUSIONS

A model for corrosion-induced cracking which combines the diffusion process and cracking process has been presented in this paper. The time-varying non-uniform corrosion distribution was obtained from diffusion analysis and effects of cover thickness and corrosion rate on the degree of non-uniformity were discussed. Concrete cover cracking under uniform and non-uniform corrosion was simulated by ATENA with discrete crack model. From this study, the following conclusions can be drawn:

1) The time-varying non-uniformity in the corrosion distribution is affected by cover thickness and corrosion rate.

2) To develop the same crack width at the cover surface, the corroded percentage of steel is lower for non-uniform corrosion than uniform corrosion. This indicates that non-uniform corrosion is more severe than uniform corrosion and should be considered in the analysis of corrosion-induced cracking.

3) The difference between results under non-uniform and uniform corrosion becomes larger with larger cover thickness, because the non-uniformity in corrosion penetration is more significant in the latter case. Proper modeling of the non-uniform rust formation is hence important for the generation of accurate results.

4) With increasing cover thickness, crack initiation on the top surface is delayed. However, once the crack is formed, it will grow faster. As a result, when corrosion-induced surface cracks are found at locations with thick cover during inspection, repair should be immediately carried out.

Table 2: Crack width evolution under non-uniform corrosion and uniform corrosion when cover is 20mm

non-uniform corrosion		
corroded depth (μm)	corroded percentage(%)	crack width (mm)
16-32	0.43	0.137
28-44	0.67	0.191
40-56	0.92	0.257
52-68	1.16	0.307
64-80	1.40	0.385
76-92	1.64	0.436

uniform corrosion		
corroded depth (μm)	corroded percentage(%)	crack width (mm)
16	0.32	0.099
24	0.48	0.138
32	0.64	0.165
44	0.88	0.225
56	1.12	0.280
64	1.28	0.338
72	1.43	0.366
80	1.59	0.406
92	1.83	0.463
100	1.99	0.497

Table 3: Crack width evolution under non-uniform corrosion and uniform corrosion when cover is 40mm

non-uniform corrosion		
corroded depth (μm)	corroded percentage(%)	crack width (mm)
0-24	0.13	-
12-44	0.45	0.204
32-64	0.85	0.328
52-84	1.26	0.452
72-104	1.66	0.568

uniform corrosion		
corroded depth (μm)	corroded percentage(%)	crack width (mm)
16	0.32	0.123
24	0.48	0.177
32	0.64	0.222
44	0.88	0.286
56	1.12	0.368
64	1.28	0.424
72	1.43	0.475
80	1.59	0.512
92	1.83	0.601
100	1.99	0.645

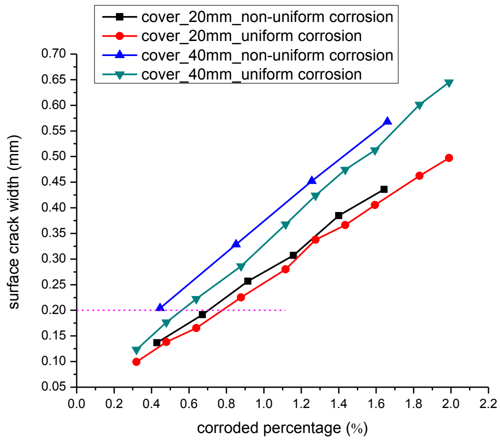

Figure 7: Relation between crack width evolution and percentage of corroded steel

REFERENCES

[1] Alonso, C., Andrade, C., Rodriguez, J. and Diez, J.M., 1998. Factors controlling cracking of concrete affected by reinforcement corrosion. *Mater. & Struct.* 31: 435-441.

[2] Molina, F.J., Alonso, C. and Andrade, C., 1993. Cover cracking as a function of rebar corrosion: Part 2—Numerical model. *Mater. & Struct.* 26:532-548.

[3] Dagher, H.J. and Kulendran, S., 1992. Finite element modeling of corrosion damage in concrete structures. *ACI Struct.* 89: 699-708.

[4] Tran, K.K., Nakamura, H., Kawamura, K. and Kunieda, M., 2011. Analysis of crack propagation due to rebar corrosion using RBSM. *Cem. &Concr. Compos.* 33: 906-917.

[5] Tran, K.K., Namamura, H., Kunieda, M. and Ueda, N. 2011. Three dimensional behaviour of concrete cracking due to rebar corrosion. *The Twelfth East Asia-Pacific Conference on Structural Engineering and Construction. Prodedia Engineering* 14: 419-426.

[6] Val, D.V., Chernin, L. and Stewart, M.G., 2009. Experimental and numerical investigation of corrosion-induced cover cracking in reinforced concrete structures. *ASCE, J. Struct. Eng.* 135: 376-385.

[7] Solgaard, A.O.S., Michel, A., Stang, H., Geiker, M.R. and Edvardsen, C. and Kuter, A., 2010. Numerical modeling of cracking of concrete due to corrosion of reinforcement-Impact of cover thickness and concrete toughness. In Oh, B.H. et al. (eds), Assessment, Durability, Monitoring and Retrofitting of Concrete Structures; *Proc. of the 7 th Inter. Conf. on Fract. Mech. of Conc. & Conc. Struct. (FraMCos-7),* May, 2010, Seoul, Korea; pp. 952-959.

[8] Du, Y.G., Chan, A.H.C. and Clark, L.A., 2006. Finite element analysis of the effects of radial expansion of corroded reinforcement. *Comp. & Struct.* 84: 917-929.

[9] Lundgren, K., 2002. Modelling the effect

of corrosion on bond in reinforced concrete. *Mag. Concr. Res.* 54: 163-173.

[10] Zhao, Y.X., Yu, J., Wu, Y.Y. and Jin, W.L., 2012. Critical thickness of rust layer at inner and out surface cracking of concrete cover in reinforced concrete structures. *Corr. Sci.* 59: 316-323.

[11] Liu, Y.P. and Weyers, R.E., 1998. Modeling the time-to-corrosion cracking in chloride contaminated reinforced concrete structures. *ACI Mater.* 95: 675-681.

[12] Oh, B.H., Kim, K.H. and Jang, B.S., 2009. Critical corrosion amount to cause cracking of reinforced concrete structures. *ACI Mater.* 106:333-339.

[13] Pantazopoulou, S.J. and Papoulia, K.D., 2001. Modeling cover-cracking due to reinforcement corrosion in RC structures. *ASCE, J. Eng. Mech.*127: 342-351.

[14] Cherin, L., Val, D.V. and Volokh, K.Y., 2010. Analytical modeling of concrete cover cracking caused by corrosion of reinforcement. *Mater. & Struct.* 43: 543-556.

[15] Ohtsu, M. and Yosimura, S., 1997. Analysis of crack propagation and crack initiation due to corrosion of reinforcement. *Constr. & Build. Mater.* 11: 437-442.

[16] Yuan Y.S. and Ji Y.S., 2009. Modeling corroded section configuration of steel bar in concrete structure. *Constr. & Build. Mater.* 23: 2461-2466.

[17] Jang B.S. and Oh, B.H., 2010. Effects of non-uniform corrosion on the cracking and service life of reinforced concrete structures. *Cem. & Concr. Res.* 40: 1441-1450.

[18] Xiao, P.W., Yi, N., Su, L.W., Li, G.B. and Wang, L.B., 2011. Finite element analysis of expansive behaviour due to reinforcement corrosion in RC structure. *2011 SREE Conference on Engineering Modeling and Simulation. Procedia Engineering*. 12 : 117-126.

[19] Zhao, Y.X., Karimi, A.R., Wong, H.S., Hu, B.Y., Buenfeld, N.R. and Jin W.L., 2011. Comparison of uniform and non-uniform corrosion induced damage in reinforced concrete based on a Gaussian description of the corrosion layer. *Corr. Sci.* 53: 2803-2814.

[20] Suda, K., Misra, S. and Motohashi, K., 1993. Corrosion products of reinforcing bars embedded in concrete. *Corr. Sci.* 35: 1543-1549.

[21] Zhao, Y.X., Ren, H.Y., Dai, H. and Jin W.L., 2011. Composition and expansion coefficient of rust based on X-ray diffraction and thermal analysis. *Corr. Sci.* 53:1646-1658.

[22] Balafas, I. and Burgoyne, C.J., 2010. Environmental effects on cover cracking due to corrosion. *Cem. & Concr. Res.* 40: 1429-1440.

[23] Kim, K.H., Jang, S.Y., Jang, B.S. and Oh, B.H., 2010. Modeling mechanical behavior of reinforced concrete due to corrosion of steel bar. *ACI Mater.* 107: 106-113.

[24] Konopka, P.2005. Structural properties of rust, Fourth-year undergraduate project, University of Cambridge.